J|A|C|S
ARTICLES
Published on Web 08/24/2002

Structural Characterization of a Paramagnetic Metal-Ion-Assembled Three-Stranded α-Helical Coiled Coil

Miriam Gochin,*,†,‡ Valentina Khorosheva,‡ and Martin A. Case§

Contribution from the Department of Pharmaceutical Chemistry, University of California San Francisco, San Francisco, California 94143, Department of Microbiology, University of the Pacific School of Dentistry, San Francisco, California 94115, and Department of Chemistry, Princeton University, Princeton, New Jersey 08544-1009

Received March 26, 2002. Revised Manuscript Received July 19, 2002

Abstract: A helical peptide designed to present an all-leucine core upon folding has been shown to exhibit concentration-dependent helicity and to exist as an ill-defined equilibrium population of oligomers. In marked contrast, an identical peptide covalently modified with a 2,2′-bipyridyl group at the N terminus forms a stable three-stranded parallel coiled coil in the presence of transition metal ions. We have employed paramagnetic Ni^{2+} and Co^{2+} ions to stabilize the trimeric assembly and to exploit their shift and relaxation properties in NMR structural studies. We find that metal-ion binding and helix-bundle folding are tightly coupled. Surprisingly, the three-helix bundle exhibits a dynamic N-terminal region, and a well-structured C-terminal half. The spectra indicate the presence of a dual conformation for the bundle extending from the N terminus to residue 12. The structure of the two isomeric forms has been ascertained from interpretation of NOEs in the Ni(II) complex and ^{1}H pseudocontact shifts in the Co(II) complex. Two different facial isomers with distinct susceptibility tensors were identified. The bulky leucine side chain at position 3 in the peptide chain appears to play a role in the conformational variation at the N terminus.

Introduction

The parallel coiled coil is an important motif in naturally occurring proteins, being implicated in protein−protein oligomerization and in the fusion machinery of enveloped viruses.[1−4] The motif is defined by a seven-amino acid repeat, the heptad repeat, in which residues *a* and *d* are hydrophobic and can form the inner core of an α-helical coiled coil or bundle. A heptad repeat sequence of fewer than 30 amino acids excised from the parent protein will not typically show well-folded behavior. However, directed assembly of the oligomeric macromolecular structure can be realized by the attachment of metal binding ligands and the addition of an appropriate metal ion.[5−7] Several groups have shown that coupling an N-terminal bidentate ligand (a 2,2′-bipyridyl group) to a peptide of an appropriate amino acid sequence can direct self-association of a parallel three-stranded α-helical coiled coil in the presence of a six-coordinate transition metal ion.[6−11] The stability of the resulting structure is dependent on details of both the metal ion/ligand chemistry and the chosen peptide sequence. Formation of the parallel coiled coil has been reported to induce selection of *facial* topological isomers at the metal center in which the three peptide chains propagate from one face of the coordinating octahedron.[8]

Despite this wealth of information, there has to date been no definitive structural characterization (either X-ray or NMR) of a designed, metal-ion-assembled three-helix bundle. Leaving aside the special problems of X-ray crystallography, multidimensional ^{1}H NMR spectra have proved difficult to interpret because of the amino acid sequence degeneracy, which causes resonances due to residues distant in sequence space to have coincident chemical shifts. To resolve this issue we speculated that the use of paramagnetic metal ions in the assembly process might allow this degeneracy to be lifted by exploiting the well-known orientational dependence of paramagnetic pseudocontact shifts.[12,13] In addition, pseudocontact shift analysis is not affected by the degeneracy of three-fold symmetry, and permits determination of the relative arrangement of individual helices within the bundle. Three *N*-bipyridylated peptides can ideally coordinate to a single paramagnetic ion such as Co(II) to create an octahedral coordination complex, for which large pseudocontact shifts and minimal dipolar line-broadening would be expected.

* Corresponding author. E-mail: miriam@picasso.nmr.ucsf.edu. Telephone: (415) 929 6442.
† University of California San Francisco.
‡ University of the Pacific School of Dentistry.
§ Princeton University.

(1) Burkhard, P. J.; Stetefeld, J.; Strelkov, S. V. *Trends Cell Biol.* **2001**, *11*, 82−88.
(2) Lupas, A. *Trends Biochem. Sci.* **1996**, *21*, 375−382.
(3) Lupas, A. *Curr. Opin. Struct. Biol.* **1997**, *7*, 388−393.
(4) Weissenhorn, W.; Dessen, A.; Calder, L. J.; Harrison, S. C.; Skehel, J. J.; Wiley, D. C. *Mol. Membr. Biol.* **1999**, *16*, 3−9.
(5) Farrer, B. T.; Harris, N. P.; Balchus, K. E.; Pecoraro, V. L *Biochemistry* **2001**, *40*, 14696−14705.
(6) Ghadiri, M. R.; Choi, C. *J. Am. Chem. Soc.* **1990**, *112*, 1630−1632.
(7) Lieberman, M.; Sasaki, T. *J. Am. Chem. Soc.* **1991**, *113*, 1470−1471.
(8) Case, M. A.; McLendon, G. L. *Chirality* **1998**, *10*, 35−40.
(9) Ghadiri, M. R.; Case, M. A. *Angew. Chem. Int. Ed.* **1993**, *32*, 1594−1597.
(10) Ghadiri, M. R.; Soares, C.; Choi, C. *J. Am. Chem. Soc.* **1992**, *114*, 825−831.
(11) Lieberman, M.; Tabet, M.; Sasaki, T. *J. Am. Chem. Soc.* **1994**, *116*, 5035−5044.
(12) Bertini, I.; Luchinat, C.; Rosato, A. *Progr. Biophys. Mol. Biol.* **1996**, *66*, 43−80.
(13) Tu, K.; Gochin, M. *J. Am. Chem. Soc.* **1999**, *121*, 9276−9285.

10.1021/ja020431c CCC: $22.00

We synthesized the peptide bpy-GELAQKLEQALQKLEQALQK-NH2 (P_{20}) according to previously published procedures,[14] as well as P_{20}-5H, with His replacing Gln at position 5, as a useful NMR probe. The bidentate ligand, bpy, is 5-carboxy-2,2′-bipyridine, tethered to the N-terminal glycine through the 5-carboxy group. The parent ligand, 2,2′-bipyridine, has an extensive and well-documented chemistry of complex formation with transition metal ions such as Ru^{2+}, Fe^{2+}, Ni^{2+}, and Co^{2+}, with which it forms octahedral tris-bipyridyl coordination complexes. The metal:peptide stoichiometry is expected to be 1:3. P_{20} contains a heptad repeat, which gives it the propensity to fold into a coiled coil structure, although the presence of Leu at both *a* and *d* positions destabilizes the parallel trimeric coiled coil in favor of states such as the dimer or an antiparallel arrangement of the helices.[15−17] This ensures that the desired tertiary structure does not form substantially in the absence of metal-ion binding, allowing us to test the design of the metal chelate−peptide complex as a parallel three-helix bundle promoter. The compatibility of metal-ion binding and helix-bundle formation was tested by CD spectroscopy and by measuring the relative binding affinities of P_{20} and P_3 for the paramagnetic metal ions Co^{2+} and Ni^{2+} using UV and NMR spectroscopy. P_3 is a truncated peptide containing only the first three residues of P_{20} and can be used to differentiate the contributions of metal chelation and peptide association to the overall stability of the complex. The P_{20} complex was found to exist in two isomeric forms by NMR spectroscopy. Theoretically, octahedral coordination with an asymmetric bidentate chiral ligand can yield up to four diastereoisomers, a meridional and facial isomer, each in either a Λ or Δ configuration. Thus, the NMR spectra of $[Ni(P_{20}\text{-}5H)_3]^{2+}$ and $[Co(P_{20}\text{-}5H)_3]^{2+}$ were analyzed to identify the isomeric composition of this system and to determine features of the three-dimensional structure and dynamics.

Experimental Section

Ni(II) and Co(II) Binding Isotherms. UV experiments were conducted on a Cary 3E UV/vis spectrophotometer. The association constants for metal binding were measured by titration of μL aliquots of concentrated metal ion into a 700 μL solution (25 mM sodium acetate, 25 mM Tris pH 7.0) of the peptide (typically 20 μM). Peptide concentrations were measured using the extinction coefficients ϵ_{291} = 12 000 and 17 500 M^{-1} cm^{-1} for P_3 and P_{20}-5H, respectively.[18] Binding was followed by recording the UV−visible spectrum from 200 to 400 nm as a function of total added metal ion. For Co^{2+} binding, it was found that the spectra at each point in the titration could be represented as a linear combination of two basis spectra, in the presence and absence of cobalt, from which the fraction of bound ligand, f_B, could be extracted. For Ni^{2+} binding, complex formation was followed by the appearance of a fairly well-resolved charge-transfer band at 313 nm. The formation of metal−ligand complexes with the bidentate bipyridyl ligands used in this study can be described by the following equilibria:

$$3L + M \overset{K_1}{\longleftrightarrow} 2L + ML \overset{K_2}{\longleftrightarrow} L + ML_2 \overset{K_3}{\longleftrightarrow} ML_3 \qquad (1)$$

The mass balance expressions for such equilibria are described by:

$$[M]_t = [M]\,(1 + \beta_1[L] + \beta_2[L]^2 + \beta_3[L]^3) \qquad (2)$$

$$[L]t = [L] + [M]\,(\beta_1[L] + 2\beta_2[L]^2 + 3\beta_3[L]^3) \qquad (3)$$

where β_i is a composite binding constant such that (for example) $\beta_2 = K_1K_2$. The population of monomeric species ML can be neglected since $K_2 \gg K_1$, leading to the binding isotherm:

$$f_B = c_1 + c_2\frac{(2\beta_2[L]^2 + 3\beta_3[L]^3)[M]_t}{[L]_t(1 + \beta_2[L]^2 + \beta_3[L]^3)} \qquad (4)$$

where f_B is the fraction of bound ligand (peptide), $[M]_t$ and $[L]_t$ are the total metal and ligand concentrations, respectively, and the free ligand concentration [L] is the positive, noncomplex root of the quartic equation in [L] resulting from the substitution of [M] from eq 2 into eq 3. c_1 and c_2 are an offset and a factor relating the basis spectrum to the fraction of complex formed. If it is further assumed that the dimeric species ML_2 can be neglected, eq 4 can be further reduced by assuming an equilibrium between free ligand and trimeric complex:

$$f_B = c_1 + c_2\frac{3[L]^3\beta_3[M]_t}{[L]_t(1 + \beta_3[L]^3)} \qquad (5)$$

The parameters c_1, c_2, β_2, and β_3 were fit by nonlinear least-squares, with the condition that c_1 and c_2 should be close to 0 and 1, respectively. Spectral decomposition and data-fitting were performed using Mathcad 8.0 (Mathsoft Engineering and Education).

Nuclear Magnetic Resonance (NMR) Experiments. One-dimensional (1D) NMR spectra were performed on a GE Omega 500-MHz spectrometer or Bruker DMX500 equipped with a standard probe. A typical spectrum of $[Co(P_{20}\text{-}5H)_3]^{2+}$ was recorded with a spectral width of 100 kHz and a delay between scans of 1 s. Concentrations of peptide used in NMR experiments varied from 2.5 to 7mM, and a pH of 6.0 was maintained using a mixture of 10 mM d_4-acetic acid and 10 mM d_{11}-Tris (Cambridge Isotope Labs). Experiments were carried out at 5 °C. T_1 relaxation times were measured by standard inversion recovery experiments. One-dimensional NOE experiments employed 20−100 ms irradiation pulses of 30−100 Hz B_1 amplitude. For chemical exchange of proton I between two sites A and B, saturation transfer results in a fractional enhancement for signal I_A caused by irradiation at I_B, given by

$$f_A(B) = k_{ex}/(R_{1A} + k_{ex}) \qquad (6)$$

where k_{ex} is the rate of conversion from A to B, and R_{1A} is the self-relaxation rate of proton I at site A. For chemical exchange involving different isomeric forms of the metal complex, k_{ex} is the off-rate of metal binding.

Two-dimensional (2D) experiments were carried out on a Varian 600 or 800 MHz machine. Experiments at 800 MHz were conducted at the Environmental Molecular Sciences Laboratory at Pacific Northwest National Labs, courtesy of Dr. Dave Lowry. Typically, a 2048 × 512 2D spectrum was collected with a spectral width of 8000−20 000 Hz and a relaxation delay of 1 s. TOCSY spectra were recorded with 30 ms or 70 ms MLEV-16 multipulse trains and 1 ms trim pulses. NOESY spectra were recorded with a mixing time of 250 ms for $[Ni(P_{20}\text{-}5H)_3]^{2+}$ and 30−100 ms for $[Co(P_{20}\text{-}5H)_3]^{2+}$. Chemical exchange in the 2D NOESY spectrum can be quantitated from the relative ratios of diagonal and cross-peak intensities. For two-site exchange with equal

(14) Case, M. A.; McLendon, G. L. *J. Am. Chem. Soc.* **2000**, *122*, 8089−8090.
(15) Bryson, J. W.; Desjarlais, J. R.; Handel, T. M.; DeGrado, W. F. *Protein Sci.* **1998**, *7*, 1404−1414.
(16) Walsh, S. T. R.; Sukharev, V. I.; Betz, S. F.; Vekshin, N. L.; DeGrado, W. F. *J. Mol. Biol.* **2001**, *305*, 361−373.
(17) Schneider, J. P.; Lombardi, A.; DeGrado, W. F. *Folding Des.* **1998**, *3*, R29−R40.
(18) Zhou, J.; Case, M. A.; Wishart, J. F.; McLendon, G. L. *J. Phys. Chem. B* **1998**, *102*, 9975−9980. (A higher extinction coefficent was consistently observed for P_{20}-5H compared to P_3.)

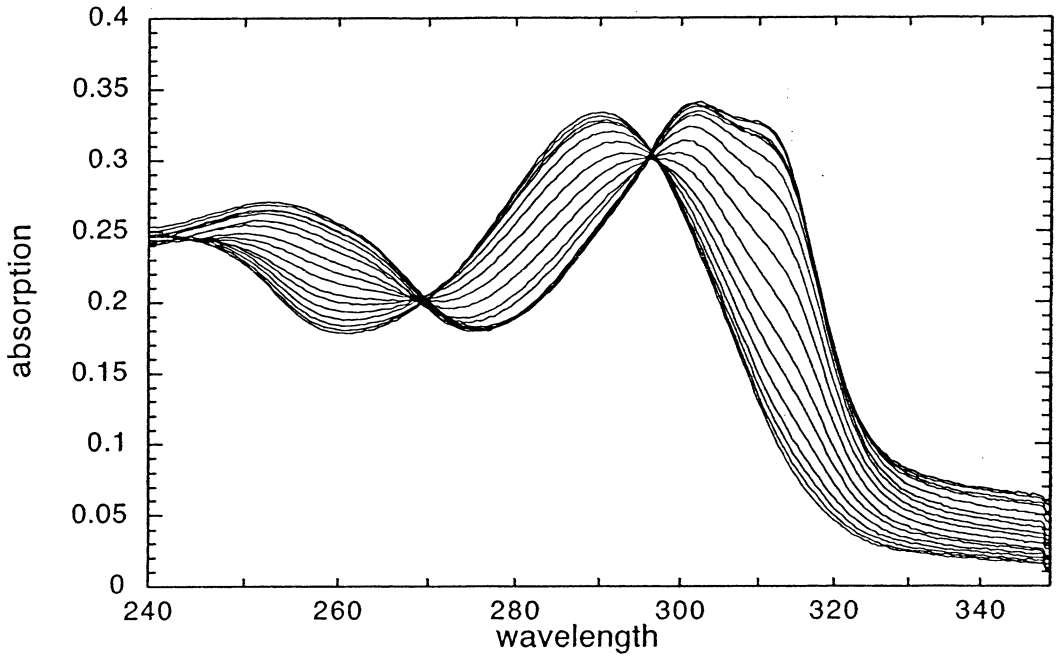

Figure 1. UV titration of $CoCl_2$ into a 20 μM solution of P_{20}-5H at pH 7 and 25 °C. Co^{2+} concentration ranged from 0.1 to 65 μM.

occupancy of both sites, this ratio is given by

$$a_{AB}/a_{AA} = (1 - \exp(-k_{ex}\tau_m))/(1 + \exp(-k_{ex}\tau_m)) \quad (7)$$

where a_{AB} and a_{AA} are the cross- and diagonal peak intensities and τ_m is the mixing time of the NOESY experiment. In the case of exchange between multiple sites, such as for $[Co(P_3)_3]^{2+}$ with four diastereoisomers, the off-rate was determined by exchange matrix analysis.[19] A 9×9 matrix was constructed, consisting of the intensities of diagonal and exchange peaks of the leucine δ_2 methyl group in free P_3 and the four bound forms of $[Co(P_3)_3]^{2+}$ in a 1:6 mixture of Co^{2+} and P_3 and diagonalized using LAPACK software to obtain the rate of Co^{2+} exchange.

Pseudocontact shifts in the NMR were calculated according to the equation

$$\delta_{pc}\ (\text{ppm}) = \{\Delta\chi_{ax}(3\cos^2\theta - 1) + 1.5\Delta\chi_{rh}\sin^2\theta\cos 2\phi\}/3r^3 \quad (8)$$

where δ_{pc} is the observed pseudocontact shift given by the difference between the shift in the Co^{2+} complex and the diamagnetic shift, $\Delta\chi_{ax}$ and $\Delta\chi_{rh}$ are the axial and rhombic magnetic susceptibility anisotropies, and (r,θ,ϕ) are the spherical polar coordinates of the observed nucleus in the principal axis system of the susceptibility tensor (PAS_χ). A best fit of observed shifts to a model structure yields values for $\Delta\chi_{ax}$ and $\Delta\chi_{rh}$ and for the orientation of PAS_χ with respect to the molecular frame of reference (Euler angles α,β,γ).

The line width in a paramagnetic system subject to exchange is given by:

$$(\pi T_{2P})^{-1} = (\pi T_{2D})^{-1} + (\pi T_{2M})^{-1} + (\pi\tau_{ex})^{-1} \quad (9)$$

where T_{2D} is the line width in the diamagnetic system, τ_{ex} is the residence time of the metal ($= k_{ex}^{-1}$), and T_{2M}^{-1} is the paramagnetic relaxation, with possible contact, dipolar and Curie contributions.[20]

Molecular Dynamics Simulations. Molecular structure calculations were carried out using a modified version of X-PLOR 3.1, which included an energy term for pseudocontact shifts.[13,21] Experimental pseudocontact shifts were calculated as the difference in observed shift for Co^{2+} and Ni^{2+} complexes, estimating the Leu3 side chain shifts in $[Ni(P_{20}\text{-}5H)_3]^{2+}$ as H_β: 1.7, H_γ: 1.6; H_δ: 0.91, 0.86 ppm. Standard all-atom force fields for proteins were used for all peptide residues, and the parameters for the bipyridyl (bpy) group were deduced from CHARM22 cofactor parameter files. To maintain planarity of the bpy groups during the simulations, van der Waal's parameters were reduced for the ring C3, C3′, H3, H3′, and nitrogen atoms. The protocol included an initial round of 300 minimization steps, followed by simulated annealing from 500 to 20 K and a second round of 500 minimization steps. Starting structures included model structures of standard helix-bundle structure and either Δ or Λ *facial* or *meridional* arrangement of the bpy groups around a central metal ion. The coordinates used were in the molecular reference frame with the metal ion at the origin, the *z*-axis along the C_{3v} symmetry axis, and the *xz* plane passing through one of the bpy nitrogen atoms. Simulations were done holding either the bpy nitrogens or the entire bpy planes fixed.

Results

The Attached Heptad Repeat Sequence Induces Higher-Affinity Metal Binding at the N-Terminal Bipyridyl Group. Figure 1 shows the spectrophotometric titration of metal ion into a 20 μM solution of P_{20}-5H. The observation of isosbestic points in the titration is indicative of a two-component mixture, that is, there is no spectroscopic evidence for the species ML or ML_2 unless their spectra are indistinguishable from that of ML_3. Titrations were analyzed according to the procedure given in Experimental Methods. Results obtained at 25 and 5 °C were virtually indistinguishable, and the 25 °C data is reported. Figure 2 shows the fit obtained for the binding of Co^{2+} and Ni^{2+} to P_3 and P_{20}-5H. Table 1 reports the parameters and binding constants resulting from fitting the data to eq 5, and in the case of Co^{2+}, to eq 4 as well. With the exception of the titration of P_3 with Co^{2+}, an excellent fit to the data could be obtained by assuming

(19) Abel, E. W.; Coston, T. P. J.; Orrel, K. G.; Sik, V. Stephenson, D. *J. Magn. Reson.* **1986**, *70*, 34−53.
(20) Bertini, I.; Luchinat, C. *NMR of Paramagnetic Molecules in Biological Systems*; Physical Bioinorganic Chemistry Series; Lever, A. B. P., Gray, H. B., Eds.; Benjamin/Cummins Publishing Co. Inc.: New York, 1986; Vol. 3.
(21) Gochin, M.; Roder, H. *Protein Sci.* **1995**, *4*, 296−305.

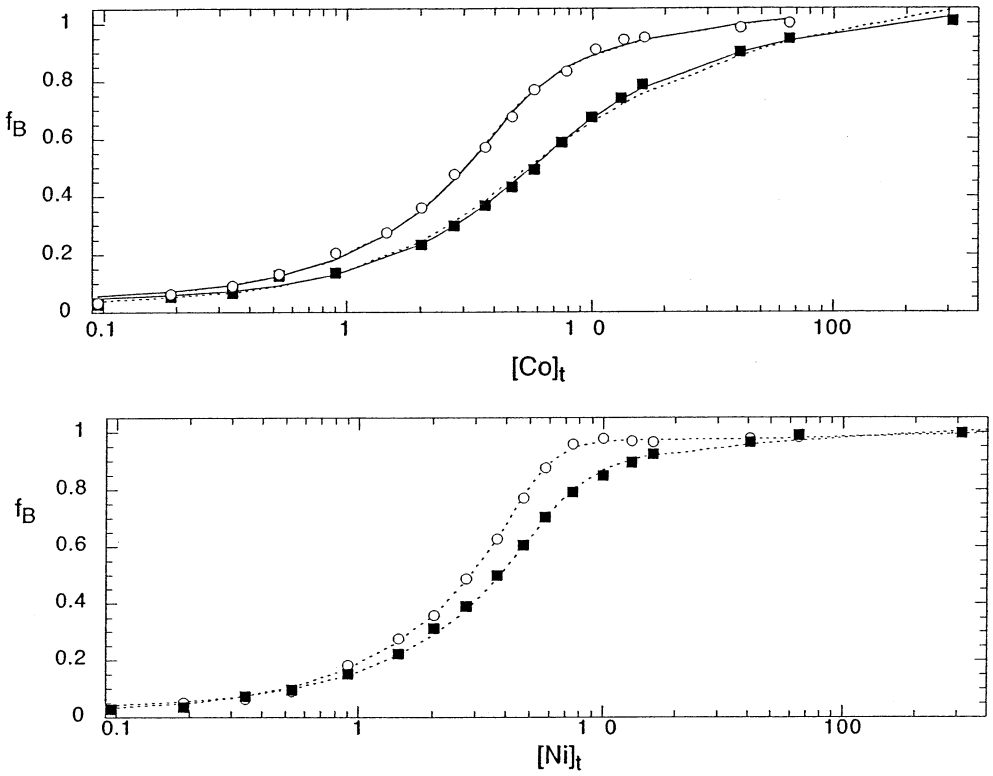

Figure 2. Fit of Co^{2+} (upper panel) and Ni^{2+} (lower panel) titrations with P_3 (■) and P_{20}-5H (○) to eq 4 (—) and eq 5 (- - -). The experimental fraction of bound ligand was determined from spectral decomposition in the case of Co^{2+} and from the intensity of the 314 nm band in the case of Ni^{2+}. For the Ni^{2+} titrations, the data could not be fit to eq 4.

Table 1. Stability Constants for Ni^{2+} and Co^{2+} Binding to P_3 and P_{20}-5H at 25 °C[a]

	$[Co(P_3)_3]^{2+}$	$[Co(P_{20}–5H)_3]^{2+}$	$[Ni(P_3)_3]^{2+}$	$[Ni(P_{20}–5H)_3]^{2+}$
β_3 (/ $10^{15}M^{-3}$)[b]	0.65 ± 0.07	16.0 ± 2.0	4.15± 0.35	43.5 ± 5.5
β_2 (/ $10^{12}M^{-2}$)[c]	0.05	0.015 ± 0.001	-	-
K_3 (/10^6M^{-1})[c]	0.013 ± 0.0014	1.09 ± 0.2	-	-
k_{off} (s^{-1})[d,e]	~1	20−70	n.d.	0.2

[a] Peptide concentrations were P_3(Co) = 26 μM, P_{20}-5H(Co) = 20 μM, P_3(Ni) = 28 μM, P_{20}-5H(Ni) = 21 μM. [b] Fit to eq 5. [c] Fit to eq 4. [d] Determined by NMR (see text). [e] Measured at 5 °C. Mean values and ranges obtained for c_1 and c_2 are 0.027 (0−0.042) and 1.11 (1.04−1.21).

only trimeric complex in solution. While this is consistent with the properties of Ni^{2+}complexes, for Co^{2+} it is known that the formation constant K_3 can be smaller than K_2, leading to a substantial population of dimer.[22] In Figure 2, the dashed lines correspond to a fit of the titrations to eq 5 (only L, ML_3 present), and the solid lines to a fit to eq 4 (L, ML_2, ML_3 species present). Both fits are superimposable for the titration of P_{20}-5H with Co^{2+}, indicating that the data is insensitive to the presence of dimer. However, the inclusion of a dimeric species gave a slightly better fit to the data in the case of P_3 with Co^{2+}. The fit to eq 4 allows β_2 and K_3 to be elucidated in addition to β_3, and these values are reported in Table 1. The Ni^{2+} titrations could only be fit to eq 5, leading to determination of β_3, but none of the composite binding constants.

P_{20}-5H has an affinity constant for Co^{2+} 25 times higher than that of P_3. Most of the effect is due to a change in the value of K_3, which is 80 times higher for P_{20}-5H than for P_3. In fact, β_2 is actually lower for P_{20} than P_3, possibly caused by strain between helix formation and optimal bipyridyl coordination

(22) Martell, A. E.; Smith, R. M. *Critical Stability Constants*; New York: Plenum Press: New York, 1974.

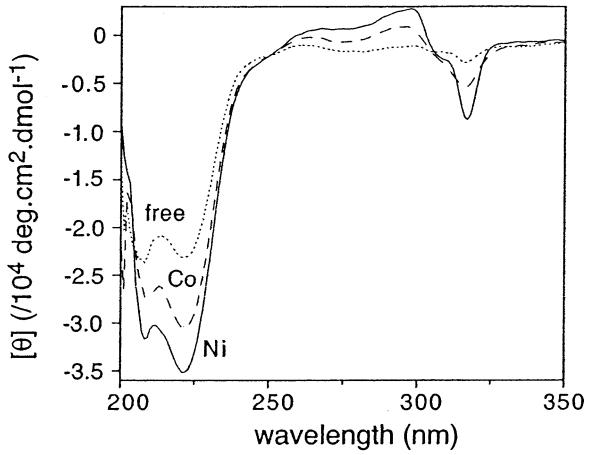

Figure 3. Circular dichroism spectra of 8 μM P_{20}, free and in the presence of 10 μM Ni^{2+} and Co^{2+}. [θ] is the mean residue ellipticity.

geometry in the dimer. The results of the UV titrations suggest that the presence of the heptad repeat peptide with an intrinsic propensity for hydrophobic collapse into a helix bundle pushes the equilibrium in favor of the trimeric species. The effect of this is to increase the apparent affinity of the metal ion for the bipyridyl ligand.

Metal-Ion Binding Induces Helix-Bundle Formation. Figure 3 shows the circular dichroism (CD) spectrum of P_{20} in the absence of metal and in the presence of Ni^{2+} and Co^{2+}. There are two features to note. First, the addition of metal ion induces a dramatic increase in the helicity of the peptides as determined by the magnitude of the ellipticity at 222 nm. Free peptide has 66% helicity, which increases to 87 and 100% in the presence of Co^{2+} and Ni^{2+}, respectively. This observation

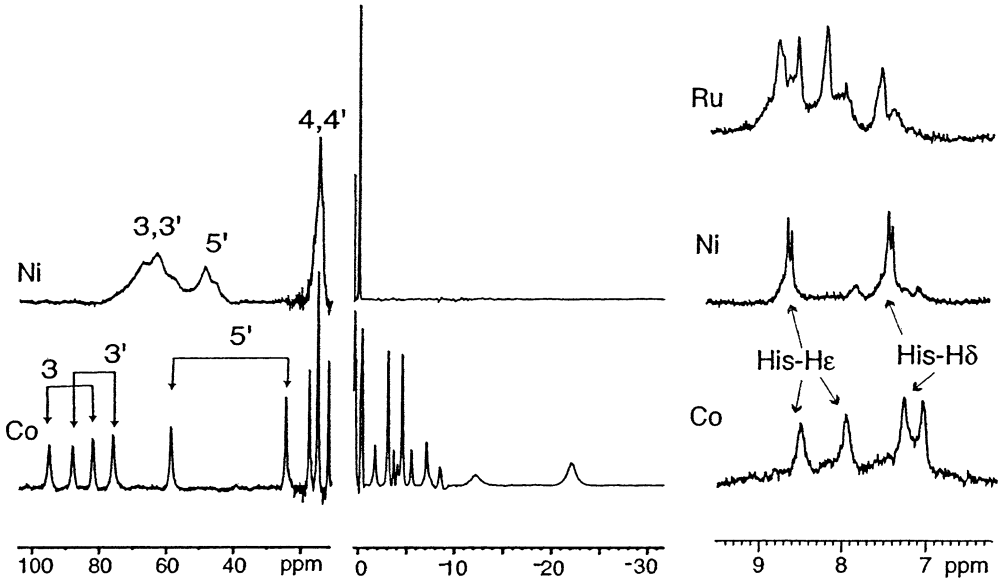

Figure 4. Aromatic and far-shifted regions of the NMR spectra of $[Ru(P_{20}\text{-}5H)_3]^{2+}$, $[Ni(P_{20}\text{-}5H)_3]^{2+}$ and $[Co(P_{20}\text{-}5H)_3]^{2+}$ taken at 500 MHz and 5 °C. The far-shifted regions of the Ni and Co complexes are shown on the left, and the expanded aromatic regions of the three metal complexes, showing His resonances as well as bpy resonances for the Ru^{2+} complex, are on the right. Assignments of the bipyridyl protons in $[Co(P_{20}\text{-}5H)_3]^{2+}$ are also indicated (see text and Figure 6).

recapitulates earlier work with similar metal-ion assembled systems. The second feature is attributed to the bipyridyl $\pi-\pi^*$ transition centered at 318 nm. The presence of this band in the CD spectrum indicates a preference for Λ over Δ stereochemistry at the metal center,[8,10,11] a result of communication of the stereogenic identity of the right-handed α-helices (possibly augmented by a left-handed supercoil) to the metal center.

^{1}H NMR Studies Using Paramagnetic Ions Verify That the Dimeric Species ML_2 Exists or Can Be Induced in Addition to the Expected ML_3 Species. The 1D NMR spectra of $[Co(P_{20}\text{-}5H)_3]^{2+}$ and $[Ni(P_{20}\text{-}5H)_3]^{2+}$ are shown in Figure 4, together with expanded aromatic regions for the Ru^{2+}, Ni^{2+}, and Co^{2+} complexes. The shifted peaks in the spectrum of $[Co(P_{20}\text{-}5H)_3]^{2+}$ are identical to those of $[Co(P_{20})_3]^{2+}$, indicating that the Q5H mutation on the solvent-exposed surface does not affect the underlying structure. The far-shifted regions of the spectrum are very sensitive to the presence of dimeric forms such as $[Ni(H_2O)_2(P_{20})_2]^{2+}$ in solution. In the spectrum of $[Ni(P_{20}\text{-}5H)_3]^{2+}$ in Figure 4, a shoulder to the right of the main peaks of bpy-H3,3′ and bpy-H5′ indicates that ∼15% dimer is present in the solution. These resonances have been identified from studies of $[Ni(P_3)_3]^{2+}$ and $Ni(bpy)_3]^{2+}$ spectra as a function of $[Ni^{2+}]$, where the equilibrium can be shifted by varying the metal:ligand ratio. Similarly, dimeric form was identified in the spectra of $[Co(P_{20}\text{-}5H)_3]^{2+}$ by the appearance of extra far-shifted peaks at Co^{2+}:P_{20}-5H ratios greater than 1:3 (Figure 5). Dimeric forms of P_3 complexes could similarly be identified by 1D NMR, at even lower than stoichiometric ratios of Co^{2+}:P_3. A comparison of the spectra of P_3 and P_{20}-5H with different Co^{2+}:peptide ratios demonstrates the effect of helix-bundle formation on the distribution of dimeric versus trimeric form (Figure 5). It is clear here, as in the analysis of UV titrations, that the heptad repeat sequence predisposes the system to form the trimeric ML_3 species over the species ML_2. This preference is not dictated by the metal ion, but rather by the hydrophobic interactions of the peptide. The equilibrium between dimeric and trimeric species can be manipulated by adjusting the relative amounts

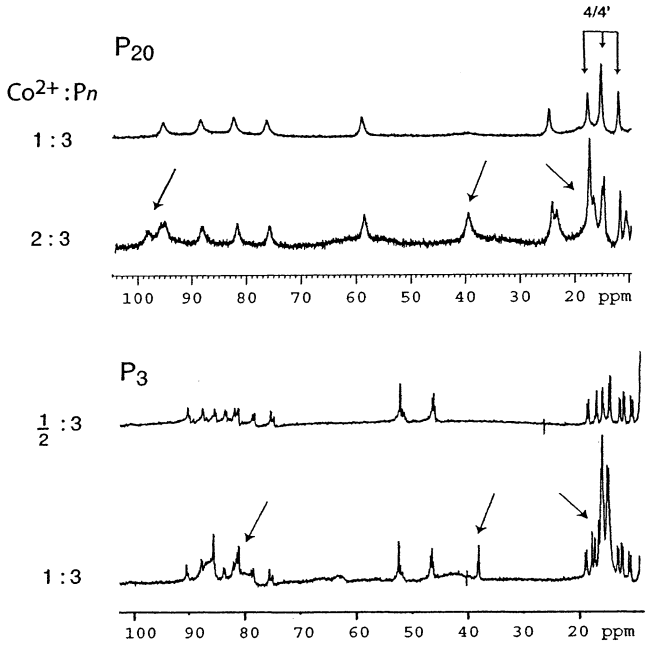

Figure 5. Comparison of the spectra of P_{20}-5H and P_3 with varying relative ratios of Co^{2+}. Arrows mark the changes in the spectra that are observed in the formation of dimeric species at higher Co^{2+}:peptide ratios.

of metal ion and ligand, and the two forms can be readily observed by NMR of the Ni^{2+} or Co^{2+} complex.

Two Isomeric Forms of the Metal Tris-bipyridyl−Peptide Complex Exist in Solution. In the diamagnetic Ru^{2+} complex, the broad bipyridyl resonances obscure the aromatic region, but in the case of Ni^{2+} and Co^{2+}, these are shifted far downfield, leaving only the resonances of the single His at position 5 in the aromatic region (Figure 4). The broad contact-shifted resonances of $[Ni(P_{20}\text{-}5H)_3]^{2+}$ and sharper contact- and pseudo-contact-shifted resonances of $[Co(P_{20}\text{-}5H)_3]^{2+}$ are consistent with the expected properties of these metal ions. The long relaxation time of the unpaired electrons on Ni^{2+} and spherical symmetry of the ground state ($^3A_{2g}$) gives rise to broad featureless contact-

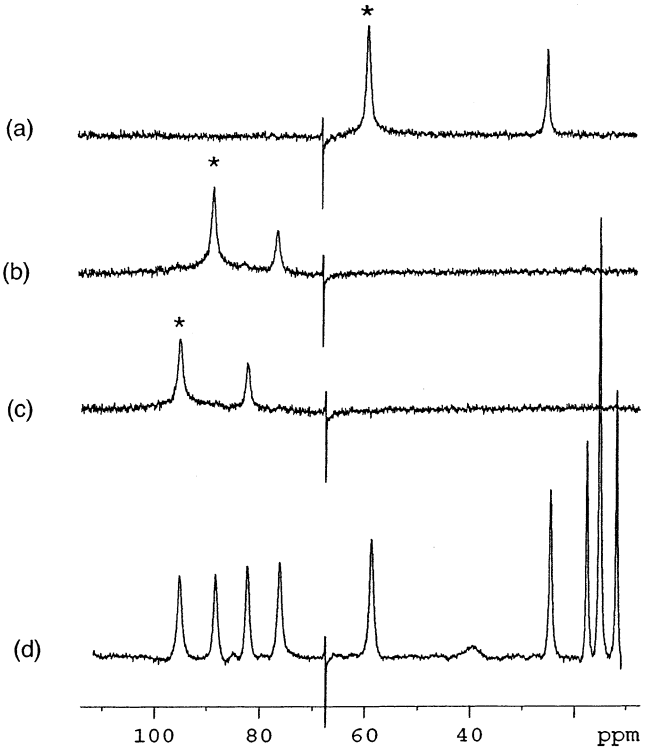

Figure 6. One-dimensional saturation transfer experiments on far-shifted bipyridyl protons. Irradiation of peaks indicated by an asterisk resulted in identification of exchange cross-peaks for (a) H5′, (b) H3′, and (c) H3 protons. Trace (d) shows the 10−110 ppm region of the spectrum for reference.

shifted resonances and the absence of pseudocontact-shifted peaks. In the case of Co^{2+}, with a $^4T_{1g}$ ground state, well-resolved widely dispersed resonances occur, with the bipyridyl resonances shifted downfield and some peptide resonances far upfield. It is immediately obvious that two isomers of the trimeric complex exist in solution in slow exchange, reflected by the appearance of two sets of resonances for the His aromatic protons and in the far-shifted regions. These are at a relative ratio of 60:40 in the Ni^{2+} complex and 50:50 in the Co^{2+} complex. One-dimensional NOE experiments on $[Co(P_{20}\text{-}5H)_3]^{2+}$ readily reveal strong chemical exchange between the two isomeric forms and the identification of resonance pairs. An example of 1D NOE assignment of resonance pairs is shown in Figure 6 for the downfield-shifted bipyridyl protons. These resonances were identified on the basis of expected chemical shifts.[23,24] Similar experiments were conducted on the upfield-shifted peptide protons. Table 2 reports the resonance assignments of the far-shifted peaks in Ni^{2+} and Co^{2+} complexes of P_{20}-5H and P_3. In contrast to the observation of two sets of resonances for $[Co(P_{20}\text{-}5H)_3]^{2+}$ and $[Ni(P_{20}\text{-}5H)_3]^{2+}$ complexes, there are eight resonances per proton readily apparent in $[Co(P_3)_3]^{2+}$, corresponding to the four allowed stereoisomers of a tris-bidentate coordination complex. There are three resonances per meridional isomer and one resonance per facial isomer, each in either a Λ or Δ configuration. Apparently, steric considerations due to helix-bundle formation restrict the allowable stereoisomers.

The isomerization implies that there are two interchanging geometries for metal-ion coordination, affecting both the chemical shifts of contact-shifted bipyridyl protons, as well as nearby peptide protons. Exchange between isomers would then likely correspond to an exchange of metal ion in and out of the complex. Further spectroscopic studies (below) revealed that the duality extends down a considerable portion of the peptide, reaching as far as residue 12.

Exchange rates between the isomeric forms were determined by 1D saturation-transfer experiments in NMR for the far-shifted resonances of $[Co(P_{20}\text{-}5H)_3]^{2+}$ and from analysis of 2D chemical exchange cross-peaks for $[Ni(P_{20}\text{-}5H)_3]^{2+}$ and $[Co(P_3\text{-}5H)_3]^{2+}$. The off-rate for Ni^{2+} binding to P_{20} was determined from the ratio of cross- and diagonal His-5 Hϵ resonances to be 0.2 s^{-1}, using eq 7. The off-rate for Co^{2+} binding to P_{20}-5H was determined by applying eq 6 to the results of 1D saturation-transfer experiments on the far-shifted resonances, giving an exchange rate on the order of 20−70 s^{-1}, about 2 orders of magnitude faster than that for Ni^{2+}. Consequently an exchange line-broadening of 10−20 Hz is expected in the spectra of $[Co(P_{20}\text{-}5H)_3]^{2+}$. These results were obtained at 5 °C. For P_3, 2D exchange matrix analysis yielded a Co^{2+} exchange rate of ∼1 s^{-1} at 25 °C. In all of these systems, the chemical exchange rates are on the order of or greater than the NOE exchange rate, which will limit the observation of NOEs between protons affected by exchange. The exchange broadening of the His aromatic protons in $[Co(P_{20}\text{-}5H)_3]^{2+}$ compared to those in nonexchanging $[Ni(P_{20}\text{-}5H)_3]^{2+}$ is 20 Hz, consistent with the observed rate of exchange. Line widths of upfield-shifted peptide resonances also show the expected line broadening, with the exception of the resonances at −22.1 and −12.2 ppm. These resonances are both over 300 Hz wide. The bipyridyl resonances have line widths that are increased by 100−450 Hz in $[Co(P_{20}\text{-}5H)_3]^{2+}$ compared to those in $[Co(P_3)_3]^{2+}$. This can be directly attributed to the large increase in Curie relaxation that occurs for the slow tumbling $[Co(P_{20}\text{-}5H)_3]^{2+}$ complex, consistent with a rotational correlation time of ∼8 ns. Such an effect, however, does not explain the line broadening of the peaks at −22.1 and −12.2 ppm, since the peptide residues are too far away to experience a large Curie effect (see below).

The NMR results demonstrate that, despite the apparently higher stability constant for metal binding to P_{20}-5H compared to P_3, the off-rate of metal binding for $[Co(P_3)_3]^{2+}$ is an order of magnitude slower than for $[Co(P_{20}\text{-}5H)_3]^{2+}$ (Table 1). The difference in affinity observed by the UV studies arises from the higher association constant for the trimeric form, which the NMR results also show to be greatly stabilized. The dimeric form of P_{20}-5H, however, is destabilized relative to that of P_3, and it acts as a conduit for metal dissociation from $[Co(P_{20}\text{-}5H)_3]^{2+}$. In addition, the hydrophobic peptide interactions prevent free diffusion of the three bpy ligands, leading to a probable on-rate for metal binding that is much larger for P_{20}-5H than P_3, to hence enhancing the apparent stability constant.

$[Ni(P_{20}\text{-}5H)_3]^{2+}$ Has α-Helical Secondary Structure and a Three-Fold Symmetry Axis. ^{1}H NMR revealed a single resonance position for each peptide proton within a given isomer, implying that there is a three-fold axis of symmetry, as expected for a three-helix-bundle structure. Furthermore, gradient diffusion studies estimate the molecular weight at ∼8 kDa, corresponding to a trimeric complex. 2D NOESY, COSY, and TOCSY spectra were recorded at 800 MHz for a solution of $[Ni(P_{20}\text{-}5H)_3]^{2+}$ at a peptide concentration of 6.5 mM. A large

(23) Huang, T. L. J.; Brewer,D. G. *Can. J. Chem.* **1981**, *59*, 1689−1700.
(24) Wicholas, M.; Drago, R. S. *J. Am. Chem. Soc.* **1968**, *90*, 6946−6950.

Table 2. Assignment of Far-shifted Resonances in Ni^{2+} and Co^{2+} Complexes of Bipyridylated Compounds, in ppm[a]

	bpy-H3	bpy-H3′	bpy-H4	bpy-H4′	bpy-H5′	leu3-Hβ	leu3Hγ	leu3Hδ
$[Ni(bpy)_3]^{2+}$	62.2	61.2	14.2	14.6	46.3	-	-	-
$[Ni(P_3)_3]^{2+}$	63.2	60.2	14.0	14.5	46.3	1.7		0.8 0.9
$[Ni(P_{20}-5H)_3]^{2+}$	67.8	63.8	15.0		49.3	n.d.	n.d.	n.d.
$[Co(bpy)_3]^{2+}$	(m): {85.4, 84.9, 82.6} (f):84.2	(m): {82.5, 81.1, 79.8} (f): 82.3	(m): {13.4, 13.9, 5.1} (f):14.8	(m):{16.0, 15.6, 14.1} (f): 14.9	(m):{48.5, 48.0, 46.4} (f):46.4	-	-	-
$[Co(P_3)_3]^{2+}$	(m): {(90.3,90.0) (87.7,87.5) (81.5,81.3)} (f): (85.5,85.3)	(m): {(75.4,74.8) (78.7,78.3) (83.6,83.4)} (f): 81.5	(m): {(10.5,10.9) (12.0,12.2) (16.0,16.1)} (f): 14.9	(m): {(18.5,18.8) (17.0,17.2) (12.7,12.9)} (f): 14.6	(m): {(51.9,51.2) (46.4,46.3) (46.3,46.1)} (f): 52.3			0.31, 0.05, −1.11, −1.45, −1.67, −2.21, −2.55, −2.68 0.24, 0.08, 0.09, −0.15, −0.23, −0.37, −0.59(2)
$[Co(P_{20}-5H)_3]^{2+}$	95.1, 82.1	88.1, 76.1	17.4, 14.8	15.2, 11.5	58.9, 24.5	−4.31, −5.75 −7.37, −8.72	−3.65,−12.22	−4.79,−22.10 4.54,−3.05

[a] Relative to internal TSP; peptides as indicated in the text, bpy = bipyridyl-5-COOH; (m) = mer, (f) = fac, numbers in parentheses are (Λ,Δ) pairs; numbers separated by commas are related by conformational exchange

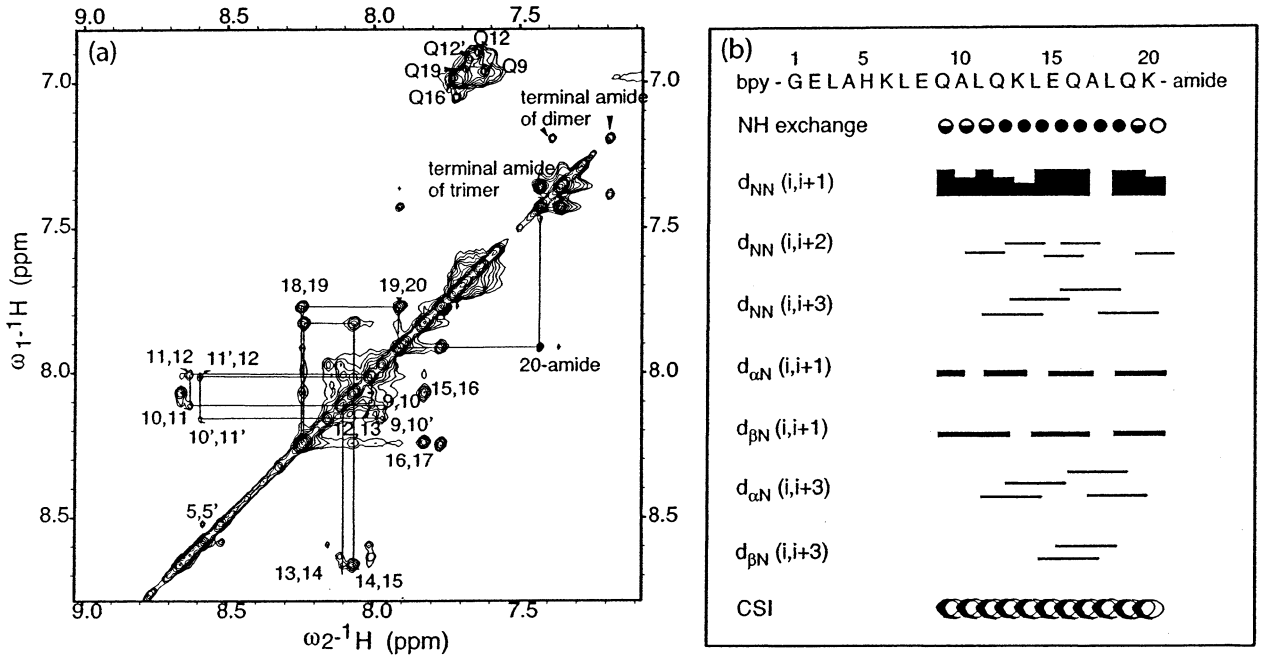

Figure 7. (a) Amide region of the 250 ms NOESY spectrum of $[Ni(P_{20}\text{-}5H)_3]^{2+}$ taken at 800 MHz. A walk through the NH−NH cross-peaks confirms helical structure for residues 9−20. Indication of dual conformers is seen in some amide positions as well as in the side chain of Q12. Also shown are terminal amide peaks considered to arise from a dimeric form of the complex. (b) Diagram of sequential and short-range NOE connectivities, hydrogen-exchange rates and consensus chemical shift index (CSI) in $[Ni(P_{20}\text{-}5H)_3]^{2+}$. Filled circles at NH exchange indicate slowly exchanging backbone amide protons estimated from the water-exchange peak intensity of the 2D NOESY. Half-filled circles indicate intermediate amide−water exchange, and unfilled circles indicate rapid exchange. The CSI defined helical structure from residues 9−20.[34] No data was obtained for the first eight residues of the complex, and the sequential $d_{NN}(i,i+1)$ connectivity between A17 and L18 could not be measured due to nearly identical shifts of these two amide protons. For residues 10−12, evidence for dual conformers was obtained in the form of peak doubling for their amide protons

underlying broad component was observed in the NOESY spectra. This is likely due to the presence of a partially unfolded peptide without a defined structure.[25] Superimposed on the broad spectrum are the sharp resonances of a folded form of $[Ni(P_{20}\text{-}5H)_3]^{2+}$ (Figure 7a). The NMR experiments were conducted at 6.5 mM peptide to favor a high population of trimeric complex. Spectra were assigned using standard procedures. Residues H5, K6, E8-K20 could be easily identified at 800 MHz despite the repetitive sequence. The assignments are reported in Table 1S of the Supporting Information. Residues G1−L3 and possibly A4 are broadened by proximity to the paramagnetic Ni^{2+}. Peak doubling of protons in residues His5 (side chain), Ala10 (NH), Leu11 (NH and side chain), and Gln12 (side chain amide) was observed. Long-range NOEs, amide proton exchange with the water and chemical shift indices of the α-^{1}H's (Figure 7b) combined to reveal a strong helical propensity for residues 9−20, but virtually no NOEs to or between the resonances of residues 5−8. The dispersion of the Leu methyl groups for L11, L14, and L18 is indicative of well-defined secondary structure.

The absence of observable NOEs for the first eight residues of the chain are indicative of a dynamic exchange occurring at or faster than the rate of the NOE transfer. The exchange involves interchange between two stereoisomers occurring at the N-terminal metal−bipyridyl complex. However, isomeriza-

(25) Fairman, R.; Chao, H.-G.; Mueller, L.; Lavoie, T. B.; Shen, L.; Novotny, J.; Matsueda, G. R. *Protein Sci.* **1995**, *4*, 1457−1469.

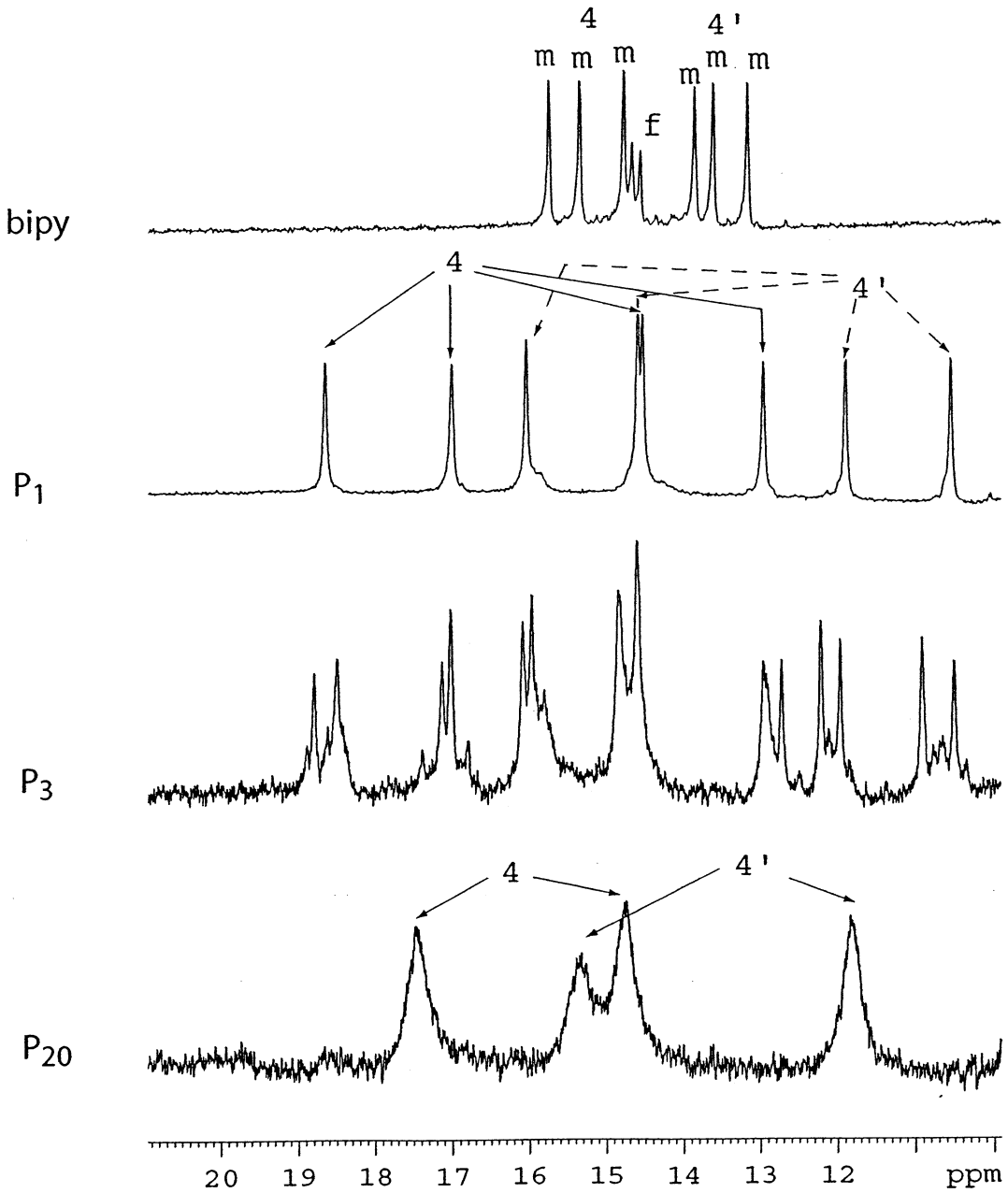

Figure 8. The bipyridyl H4,H4′ region of the spectra of $[Co(bpy)_3]^{2+}$, $[Co(P_1)_3]^{2+}$, $[Co(P_3)_3]^{2+}$, and $[Co(P_{20})_3]^{2+}$ indicating the sensitivity of the spectra to diastereoisomerization. m = *meridional*, f = *facial* isomer.

tion is leading to changes more than halfway down the helix bundle and would seem to imply that a rather large conformational change exists between the two isomeric forms. It is hard to conceive, for example, of a simple Λ, Δ switch that would require such a rearrangement of the bundle structure.

It was also possible to identify the peaks due to the dimeric form in the 2D spectra. NOEs consistent with a second helix could be identified for the C-terminal resonances -ALQK-amide, and additional weak unidentified resonances considered to arise from the dimer occurred in the αH and methyl regions of the NOESY. From the relative intensities of the amide resonances in the dimeric and trimeric forms, the dimer was found to be populated by 14%.

Pseudocontact Shifts in $[Co(P_{20}\text{-}5H)_3]^{2+}$ Reveal the Nature of the Two Isomers. The Co^{2+} complex is ideally suited for studying the N-terminal region of the helix bundle because of the high sensitivity of the pseudocontact shift to structure close to the metal ion. A clue to the identity of the two isomeric forms comes from a comparison of the shift differences between their respective resonances in $[Co(P_{20}\text{-}5H)_3]^{2+}$. The effect of substitution of the chiral peptide on the bipyridyl resonances can be gauged by comparison of the spectra of $[Co(bpy)_3]^{2+}$, $[Co(P_1)_3]^{2+}$, $[Co(P_3)_3]^{2+}$, and $[Co(P_{20})_3]^{2+}$ in Table 2 and Figure 8. The ligands bpy and P_1 are 5-carboxybipyridine and bpy-gly-amide respectively, both of which have nonchiral substituents on the ring. The result of peptide substitution (i.e., gly addition to bpy) is to spread the range of observed resonances of a particular proton in the various stereoisomers from ∼2 to up to 7 ppm. The Δ,Λ diastereoisomerization induced by the chiral substituent in P_3, causes a further 0.2−0.3 ppm split in the resonances. In P_{20}, the number of observable isomers has

Table 3. Comparison of Observed and Calculated Leu3 and His5 Side Chain Pseudocontact Shifts for the Two Conformations of $[Co(P_{20}\text{-}5H)_3]^{2+}$

	observed[a]	calculated[a,c]	distance[a,d]	observed[b]	calculated[b,c]	distance[b,d]
Leu3 Hβ1	−7.45	−7.08 (0.17)	10.42	−6.01	−5.21 (0.17)	8.40
Leu3 Hβ2	−10.42	−10.89 (0.10)	9.98	−9.07	−9.34 (0.05)	7.92
Leu3 Hγ	−13.82	−13.67 (0.23)	8.19	−5.25	−4.90 (0.08)	6.58
Leu3 Hδ1	−23.01	−22.88 (0.15)	7.53	−5.70	−6.40 (0.05)	5.89
Leu3 Hδ2	−3.91	−4.25 (0.11)	8.80	3.68	3.13 (0.06)	8.00
His5 Hδ2	−1.13	−1.65 (0.29)	14.00	−1.38	−1.87 (0.16)	12.47
His5 Hϵ1	1.63	1.52 (0.57)	12.83	1.11	0.36 (0.11)	11.73

[a] Conformer A, calculated with $\Delta\chi_{ax} = 11100$ ppmÅ^3. [b] Conformer B, calculated with $\Delta\chi_{ax} = 6600$ ppmÅ^3. [c] Averaged over the three peptide chains with the standard deviation shown in brackets. [d] Distance from metal ion.

reverted to two, and the lines are considerably broadened by Curie relaxation.

Shift variations of a similar magnitude are observed for H3, H3′, and H5′ protons between bpy, P_1, and P_3 complexes. By contrast, the difference in H5′ resonance positions for the two isomeric forms of $[Co(P_{20}\text{-}5H)_3]^{2+}$ is 30 ppm (Table 2). The magnitude of the effect cannot be accounted for simply by diastereoisomerization, because of limitations imposed upon Δ and Λ related susceptibility anisotropy tensors. Left- and right-handed tensors must be related by a simple negation of angles defining their orientation with respect to the molecular reference frame, and calculations show that subsequent changes in pseudocontact shift are limited to less than 1 ppm. This calculation is borne out by the small stereochemical effect observed in the spectra of $[Co(P_3)_3]^{2+}$. Changes in contact shift as a result of change in stereochemistry are also expected to be negligible, and this is corroborated by comparison of contact shifts in Ni^{2+} complexes $[Ni(bpy)_3]^{2+}$, $[Ni(P_3)_3]^{2+}$, and $[Ni(P_{20}\text{-}5H)_3]^{2+}$ (data not shown). The fact that only one pseudocontact-shifted resonance occurs per bipyridyl proton per isomer also indicates that three-fold symmetry must occur throughout the complex and that meridional forms of metal coordination do not occur.

A similarly large chemical shift difference between the two isomeric forms in $[Co(P_{20}\text{-}5H)_3]^{2+}$ was observed for the upfield-shifted methyl groups of Leu3, which appear as a set of eight resonances per methyl group in $[Co(P_3)_3]^{2+}$ and as a pair of resonances per methyl group in $[Co(P_{20}\text{-}5H)_3]^{2+}$. Resonance assignments were made from chemical exchange cross-peaks between free and bound P_3, or from observed TOCSY and NOESY correlations between side chain protons of Leu3 in $[Co(P_{20}\text{-}5H)_3]^{2+}$. The chemical shift spread of the Leu3 δ1 and δ2 methyl groups over the eight resonances in $[Co(P_3)_3]^{2+}$ covers 3 and 0.8 ppm, while the resonance pairs of the two methyl groups in $[Co(P_{20}\text{-}5H)_3]^{2+}$ are 17.6 and 9 ppm apart, respectively. Again this implies a structural difference between the two isomers of $[Co(P_{20}\text{-}5H)_3]^2$, exceeding a simple Δ,Λ mixture. Since the pseudocontact shifts are directly related to structure, we have been able to use the shifts of the Leu3 side chain protons in a least-squares analysis against various model structures to identify those in compliance with the observed shifts. A molecular dynamics simulation was carried out using each set of Leu3 and His5 side chain pseudocontact shifts as constraints (See Experimental Methods). The results are shown in Table 3 and Figure 9. From various starting structures, the side chain of the Leu3 converged to the two positions illustrated in Figure 9 with a good agreement to the two observed pseudocontact shifts data sets. An exception to this is the Hϵ1 proton pseudocontact shift, which could not be accurately

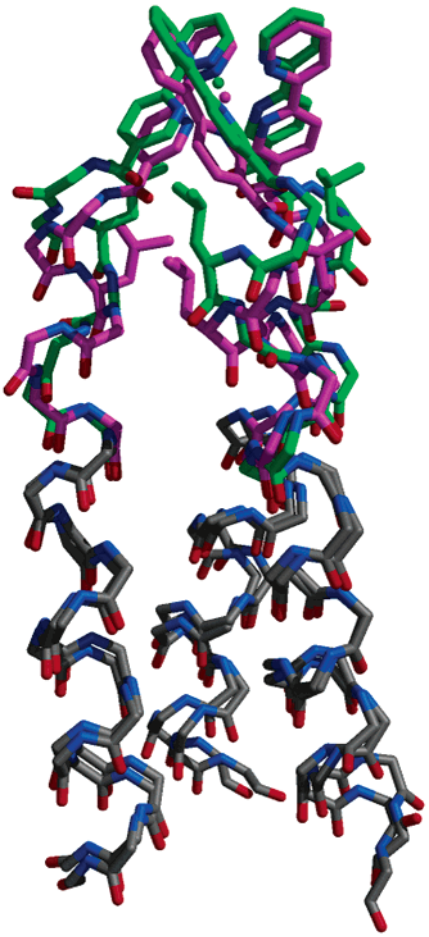

Figure 9. Superposition of conformers A and B arising from pseudocontact shift analysis and molecular dynamics simulations of $[Co(P_{20}\text{-}5H)_3]^{2+}$ (see text). The two structures were superimposed from residues 13−20, in accordance with experimental observations of a unique structure for this region. Only the backbone, bipyridyl group, metal ion, and Leu3 side chain are shown. The carbon atoms of residues 1−12 are shown in magenta and green, respectively, for conformers A and B.

reproduced. Due to the sensitivity of this shift to pH fluctuations between samples, it was weighted less heavily during the simulations. Accompanying the two side chain orientations are two distinct conformations of the backbone and surrounding side chains required to accommodate a low-energy structure while keeping the bipyridyl−metal coordination intact. The conformational variation between the two forms, A and B, extends all the way down to Gln12, explaining the NMR results for $[Ni(P_{20}\text{-}5H)_3]^{2+}$.

Accurate susceptibility anisotropy tensors cannot be obtained from the structure calculations for a number of reasons. The small number of pseudocontact shifts available and the fact that

they correspond to side chain positions only limits the reliability of the tensors derived. In addition, diamagnetic shifts were estimated from the spectrum of $[Ni(P_{20}\text{-}5H)_3]^{2+}$ but not directly observed, limiting the accuracy of the shift data set. Nevertheless, some important features of the tensors were obtained. With the molecular *z*-axis defined as the pseudo-three-fold symmetry axis running down the length of the helix bundle, with the metal ion at the origin, symmetry considerations result in the condition that $\Delta\chi_{rh} = -2\Delta\chi_{ax}$, which implies that $\Delta\chi_{zz} = \Delta\chi_{yy}$. The Euler angles α, β, γ which define the relative orientation of the tensor and molecular reference frames are, respectively, undefined, 90° and 90°, implying that the *z*-axis of the susceptibility anisotropy tensor is perpendicular to the axis of symmetry and along the molecular *y* axis. The angle α is undefined because of the equivalence of $\Delta\chi_{zz}$ and $\Delta\chi_{yy}$. It appears that the size of the susceptibility anisotropy is different for the two conformers. The pseudocontact shift conditions could be met with a range of values of $\Delta\chi_{ax}$, although the best fit was obtained with a value of 11100 and 6600 ppm·Å^{-3} for conformers A and B, respectively, and these results are reported in Table 3. A full structural analysis will be the subject of another paper.

Discussion

The peptide P_{20}-5H forms a three-stranded helical bundle structure with an all-leucine core in the presence of transition metal ions. Extensive protein design studies[26−33] on unmodified peptides have determined that the relatively bulky leucine side chains do not form a well-packed interior with discrete rotameric states, but rather a fluid molten globular core.[15,17] This results in a helix bundle that is only marginally stable and does not fold cooperatively. The effect of metal-ion addition to the bipyridylated peptide is to substantially stabilize the helix bundle. NMR spectra contain a considerable broad featureless component, underlying the sharp resonances of a well-folded construct, which must be due to the partial dissociation of the complex. The properties of the bundle are dictated more by the peptide sequence than by the N-terminal metal-ligation complex. In fact, the lability of metal coordination leads to substantial fluctuation of the structure at the N-terminal end. However, metal binding appears to contribute to the overall stability of the complex. The propensity of P_{20} to form a three-helix bundle contributes to a redistribution of dimeric versus trimeric form of metal−bipyridyl ligation. Thus, while a considerable amount of dimer is observed with P_3 above Co^{2+}:P_3 ratios of 1:6, no dimer is observed with P_{20}-5H below the stoichiometric Co^{2+}:P_{20}-5H ratio of 1:3. Concomitantly, the equilibrium constant K_3, for the formation of metal-tris-bipyridyl complex is significantly larger for $[Co(P_{20}\text{-}5H)_3]^{2+}$ than for $[Co(P_3)_3]^{2+}$.

Solution NMR studies on Ni and Co complexes have demonstrated that the overall structural properties are the same for these two metal ions. The trimeric complex exists in two detectable isomeric forms, which involve a structural reorganization that extends more than halfway down the helix. Peak doubling in $[Ni(P_{20}\text{-}5H)_3]^{2+}$ is seen as far as Q12. The exchange rate of the Ni^{2+} ion, 0.2 s^{-1}, affects the observation of NOEs in the first part of the helix. However, evidence of helical structure for this region was obtained from the observed paramagnetic shifts and line broadening of the His5 aromatic protons in $[Co(P_{20}\text{-}5H)_3]^{2+}$. Paramagnetic shift calculations put the His5 aromatic protons between 12 and 14 Å from the metal ion, in accordance with a helical backbone structure at the N terminus. Thus, the N-terminal region of the bundle appears to be dynamic but not disordered.

The properties of the NMR spectrum of $[Co(P_{20}\text{-}5H)_3]^{2+}$ provide some insight into the nature of the conformational fluctuation. Calculations have shown that we cannot distinguish between Λ and Δ forms of a particular stereoisomer at the current level of resolution. The effect of a change in handedness alone at the metal coordination would not be expected to dramatically affect the resonances of the peptide. However, it should be clearly observed in resonances of the bipyridyl group, as it clearly is in the spectrum of $[Co(P_3)_3]^{2+}$. However, the large line width of the bipyridyl resonances in $[Co(P_{20}\text{-}5H)_3]^{2+}$, shifted out of the main spectral envelope and lying between 12 and 100 ppm, precludes the observation of the small 0.2−0.3 ppm shift differences expected between Λ and Δ diastereoisomers. Thus, one observed resonance may encompass signals of both Λ and Δ diastereoisomers. The resonances of the H4 and H4′ protons in Figure 8 illustrate this effect. The line width of these resonances in $[Co(P_{20}\text{-}5H)_3]^{2+}$ covers the range of the observed Λ/Δ splitting in resonances of $[Co(P_3)_3]^{2+}$ and could be representative of the presence of both diastereoisomers that are simply not resolved.[8]

Instead, the two conformations appear to correspond to structurally different molecules, conformers A and B, both facial enantiomers, each represented by a different susceptibility anisotropy tensor. The large difference in pseudocontact shifts consequently incurred is sufficient to explain the large chemical shift difference of far-shifted resonances between the two structural forms. What is not understood, however, is the very large line widths of the leucine-3 Hδ1 and Hγ protons of conformer A, which significantly exceed expected line widths by as much as 200 Hz. It is possible that the magnetic susceptibility anisotropy may play a role in the relaxation behavior of these resonances.

Co^{2+} exchanges 10 times as fast in $[Co(P_{20}\text{-}5H)_3]^{2+}$ compared to $[Co(P_3)_3]^{2+}$. This result implicates the bundle structure as causing distortion of the ideal octahedral geometry of a tris-bipyridyl−metal complex. Indeed, in the final structures obtained by simulated annealing, deviations from ideal geometry occur and are restricted to the configuration around the bipyridyl carboxyl carbon and glycine amide nitrogen. The selection of the linkage bpy-GEL to couple the metal coordination to the helix bundle is probably not optimal. The Leu3 side chain is bulky and may be the cause of the two distinct conformations. The affinity of the metal ion is further degraded by substitution of the electron-withdrawing carboxyl group at position 5 (also present in $[Co(P_3)_3]^{2+}$) and by the helix dipole effect which creates a net positive charge at the N-terminal end.

(26) Beasley, J. R.; Hecht, M. H. *J. Biol. Chem.* **1997**, *272*, 2031−2034.
(27) Hodges, R. S.; Saund, A K.; Chong, P. C. S.; St. Pierre, S. A.; Reid, R. E. *J. Biol. Chem.* **1981**, *256*, 1214−1224.
(28) Kohn, W. D.; Hodges, R. S. *Trends Biotechnol.* **1998**, *16*, 379−389.
(29) Munson, M.; Balasubramanian, S.; Fleming, K. G.; Nagi, A. D.; OBrien, R.; Sturtevant, J. M.; Regan, L. *Protein Sci.* **1996**, *5*, 1584−1593.
(30) Regan, L.; DeGrado, W. F. *Science* **1988**, *241*, 976−978.
(31) Zhou, N. E.; Zhu, B.-Y.; Kay, C. M.; Hodges, R. S. *Biopolymers* **1992**, *32*, 419−426.
(32) Micklatcher, C.; Chmielewski, J. *Curr. Opin. Chem. Biol.* **1999**, *3*, 724−729.
(33) Woolfson, D. N. *Curr. Opin. Struct. Biol.* **2001**, *3*, 724−729.
(34) Wishart, D. S.; Sykes, B. D.; Richards, F. M. *Biochemistry* **1992**, *31*, 1647−1651.

The C terminus of $[Ni(P_{20}\text{-}5H)_3]^{2+}$ is surprisingly well-structured for such a short peptide. Good dispersion of NMR resonances and a clear helical pattern for the NOEs occur despite the repetitive sequence. This dispersion, as well as discreet NOE contacts, includes the three leucine residues at positions 11, 14, and 18, which may indicate that these side chains do in fact adopt a discrete structure and that the bundle is well-folded. Accordingly, CD results suggest a high degree of helical structure, although they are not sensitive to the dynamic properties seen in the NMR.

These results show that the formation of the helix bundle and the binding of metal ion to the N-terminal bidentate bipyridyl ligands are processes that are highly cooperative, and in this way the design criteria have been fulfilled. Future steps can be taken to improve the design, particularly by alteration of the bpy−peptide linker.

Acknowledgment. This work was supported by Grants NIH 53164 and the UniversityWide AIDS Research Project R00-UP-092 to M.G., and by Grant CHE-0106342 (National Science Foundation Division of Chemistry) to M.A.C.. M.G. is indebted to Dr. Dave Lowry at the Environmental Molecular Sciences Laboratory at Pacific Northwest National Labs for the acquisition of spectra obtained at 800 MHz. We are grateful to Dr. Ivan Smirnov and Professor Richard Shafer for invaluable discussions. UV, CD, and NMR spectrometers were available as shared resources in the Departments of Pharmaceutical Chemistry and Biophysics at UCSF.

Supporting Information Available: Table of chemical shifts of assigned residues (PDF). This material is available free of charge via the Internet at http://pubs.acs.org.

JA020431C